

Kinetic Resolution of Allylic Alcohol with Chiral BINOL-based Alkoxides: A Combination of Experimental and Theoretical Studies

Yidong Liu, Song Liu, Dongmei Li, Nan Zhang, Lei Peng, Jun Ao, Choong Eui Song, Yu Lan, and Hailong Yan

J. Am. Chem. Soc., **Just Accepted Manuscript** • DOI: 10.1021/jacs.8b12796 • Publication Date (Web): 18 Dec 2018

Downloaded from <http://pubs.acs.org> on December 27, 2018

Just Accepted

“Just Accepted” manuscripts have been peer-reviewed and accepted for publication. They are posted online prior to technical editing, formatting for publication and author proofing. The American Chemical Society provides “Just Accepted” as a service to the research community to expedite the dissemination of scientific material as soon as possible after acceptance. “Just Accepted” manuscripts appear in full in PDF format accompanied by an HTML abstract. “Just Accepted” manuscripts have been fully peer reviewed, but should not be considered the official version of record. They are citable by the Digital Object Identifier (DOI®). “Just Accepted” is an optional service offered to authors. Therefore, the “Just Accepted” Web site may not include all articles that will be published in the journal. After a manuscript is technically edited and formatted, it will be removed from the “Just Accepted” Web site and published as an ASAP article. Note that technical editing may introduce minor changes to the manuscript text and/or graphics which could affect content, and all legal disclaimers and ethical guidelines that apply to the journal pertain. ACS cannot be held responsible for errors or consequences arising from the use of information contained in these “Just Accepted” manuscripts.

Kinetic Resolution of Allylic Alcohol with Chiral BINOL-based Alkoxides: A Combination of Experimental and Theoretical Studies

Yidong Liu,^{†,‡} Song Liu,^{#,‡} Dongmei Li,[†] Nan Zhang,[†] Lei Peng,[†] Jun Ao,[†] Choong Eui Song,[§] Yu Lan,^{*,#} and Hailong Yan^{*,†}

[†]Chongqing Key Laboratory of Natural Product Synthesis and Drug Research, School of Pharmaceutical Sciences and [#]School of Chemistry and Chemical Engineering, Chongqing University, Chongqing 400030, P. R. China

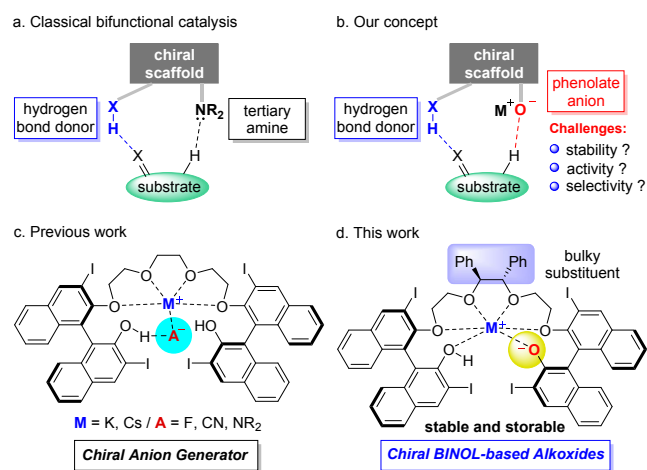
[§]Department of Chemistry, Sungkyunkwan University, 2066, Seobu-ro, Jangan-gu, Suwon, Gyeonggi 440-746, Korea

ABSTRACT: The development and characterization of enantioselective catalytic kinetic resolution of allylic alcohols through asymmetric isomerization with chiral BINOL derivatives-based alkoxides as bifunctional Brønsted base catalyst were described in the study. A number of chiral BINOL derivatives-based alkoxides were synthesized and their structure-enantioselectivity correlation study in asymmetric isomerization identified a promising chiral Brønsted base catalyst, which afforded various chiral secondary allylic alcohols (ee up to 99%, *s* factor up to >200). In the mechanistic study, alkoxide species were identified as active species and the phenol group of BINOL largely affected the high reactivity and enantioselectivity via hydrogen bonding between the chiral Brønsted base catalyst and substrates. The strategy is the first successful synthesis strategy of various chiral secondary allylic alcohols through enantioselective transition-metal-free base catalyzed isomerization. The applicability of the strategy had been demonstrated by the synthesis of bioactive natural product (+)-veraguensin.

INTRODUCTION

Catalysis is one of the central themes in science. Therefore, the design and application of new, efficient types of catalysts are of fundamental importance.¹ Recently, the development of a new type of chiral Brønsted base catalyst has received considerable attention since a range of important classes of organic reactions can be promoted with a Brønsted base.² Brønsted bases can accept a hydrogen (or proton) from an acidic source or equivalent activated species. This proton transfer forms the basis of the key activation component in the formations of new chemical bonds. However, the intrinsic nature of the ion pairing complex of Brønsted bases can become a challenge in stereoinduction, especially when the starting reagents are achiral. The catalyst with a Brønsted base moiety and another site with hydrogen-donating characteristics becomes a bifunctional Brønsted base catalyst³ that can overcome the stereoinduction problems. In such a way, the Brønsted base catalyst has gained the ability to stabilize both nucleophile and electrophile in the transition state. In the past two decades, new bifunctional Brønsted base catalysts, especially the catalysts containing nitrogen as a Brønsted base moiety and hydrogen bonding moieties (XH group), have been significantly improved due to mechanism studies and insightful observations about Brønsted base and hydrogen bond donor activation of substrates (Scheme 1a).

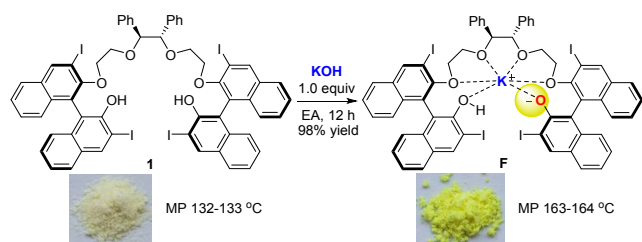
Scheme 1. Design of a Brønsted Basic Bifunctional Catalyst Containing Phenolate Anion as a Brønsted Base Moiety



1,1'-Bi-2-naphthol (BINOL)⁴ is the common core skeleton of the catalyst in asymmetric synthesis. Due to the acidity of phenolic protons, BINOLs are often used as Brønsted acid and/or hydrogen bond donor in asymmetric catalysis. However, according to the Brønsted-Lowry theory,⁵ the deprotonation of BINOLs will occur at high pHs and give the phenolate anion (also called phenoxide), which can act as the Brønsted base in many reactions theoretically. In addition, the availability of an additional phenol group of BINOL moiety offers the stronger stereogenic-tuning to the activated and

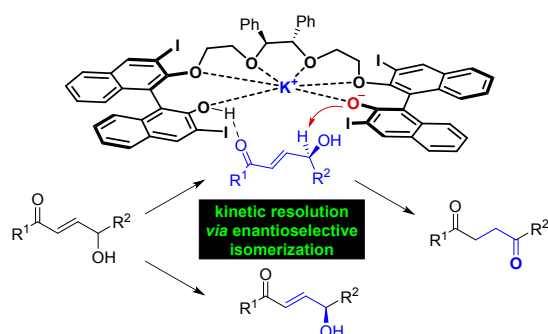
stabilized transition state through the hydrogen bonding. However, due to the lack of the strategy to stabilize the phenolate anion, a bifunctional binaphtholate catalyst was seldom reported. Furthermore, all the reported binaphtholate catalysts were in-situ generated with strong alkali metal bases.⁶ Thus, it is necessary to develop a stable and storable bifunctional binaphtholate catalyst for both enriching the classes of catalysts and exploiting new synthetic strategies (Scheme 1b).

Scheme 2. Preparation of Chiral BINOL Derivatives-based Alkoxides



Recently, we reported an easily accessible 1,1'-bi-2-naphthol (BINOL)-based bis(hydroxy) polyethers bearing phenols and polyether units for asymmetric cation-binding catalysis.⁷ The ether oxygens act as a Lewis base to coordinate metal ions such as K^+ , thus generating a soluble chiral anion, which can be used as the base or nucleophile in a confined chiral space. This new type of cooperative cation-binding catalysis had been successfully applied in various asymmetric reactions (Scheme 1c). Inspired by these advancements, we envisioned a complementary strategy, which represented a different approach to expand the scope of this novel catalyst. In principle, if we treated our catalyst with alkali metal salts such as KOH , and K_2CO_3 , a chiral BINOL derivatives-based alkoxide would be generated. In the reaction, K^+ might play a crucial role in stabilizing the phenolate anion. A family of robust 1,1'-bi-2-naphthol (BINOL)-based alkoxides were prepared. Especially, catalyst F with the substituents at the C_1 position of the chain was prepared for the first time (Scheme 1d, 2). The prepared chiral alkoxides had the high solubility in organic solvents and were insensitive to water and air. The study aims to evaluate this novel strategy and present a new chiral

Scheme 3. Asymmetric Isomerization of Allylic Alcohols Using Chiral BINOL Derivatives-based Alkoxides



alkoxide catalyst for the kinetic resolution of range of racemic allylic alcohol via enantioselective isomerization⁸ (Scheme 3). Notably, the catalyst's Brønsted base component (phenolate anion) is identified as a basic unit required for the catalytic activity, involving a base-promoted proton abstraction as the activation step. The chemistry to be detailed was enabled by a seemingly trivial, yet ultimately crucial deviation from established art in asymmetric catalysis.

The catalytic isomerization of allylic alcohols represents a useful synthetic process to generate aldehydes or ketones. In the development of the catalytic enantioselective variant of this process, great advancements had been achieved in the isomerization of β -substituted primary allylic alcohols since the pioneering reports by the Fu group,⁹ the Mazet group¹⁰ and others.¹¹ As for the corresponding secondary allylic alcohols, only a few kinetic resolution¹² of racemic alcohols¹³ or stereospecific isomerization of enantioenriched substrates¹⁴ to β -substituted ketones had been reported. Recently, Zhao¹⁵ made a landmark achievement in Rh-catalyzed enantioselective isomerization of secondary allylic alcohols. In particular, this work represents the first enantioselective redox-neutral synthesis of ketones with an α -tertiary stereocenter. In addition, enantiopure allylic alcohols are versatile building blocks for asymmetric synthesis and widely exist in complex natural products.¹⁶ Their utility has been largely demonstrated in a variety of organic transformations. Due to the importance of allyl alcohol in organic synthesis, in our preliminary study, we chose racemic (*E*)-4-hydroxy-1,4-diphenylbut-2-en-1-one (\pm)-**2a** as the model substrate. The deprotonation of allylic C-H easily occurred under mild basic conditions and then the isomerization proceeded logically.

RESULTS AND DISCUSSION

To verify the feasibility of the proposed process, a range of potential catalysts, including chiral bifunctional catalysts **A-D**¹⁷ and chiral BINOL derivatives-based alkoxides **E-G**, were tested in the resolution of (\pm)-**2a** (Table 1). In order to amplify potentially subtle differences among the catalysts, the reactions were performed under a catalyst load of 10 mol% at room temperature in *o*-xylene and then quenched after 3 h. Under the above conditions, chiral thiourea catalysts **A-C** showed the poor selectivity (Table 1, entries 1-3). Surprisingly, quinine-derived squaramide **D** provided a satisfactory *s* factor of 13 (31% conversion), but the reaction proceeded sluggishly (Table 1, entry 4).

Next, we screened the catalytic efficiency of a variety of chiral BINOL derivatives-based alkoxide catalysts to shed light on the relationship between the structures of catalysts **E-G** and reaction outcomes. As shown in Table 1, entry 5, when catalyst **E1** having no substituent at the 3,3'-position on the BINOL group was employed, a very low level of conversion and enantioselectivity were observed. However, the introduction of the substituents such as CH_3 (**E2**), CF_3 (**E3**) and I (**E4**) on the 3,3'-positions of

Table 1. Catalyst Screening and Optimization of Reaction Conditions^a

1
2
3
4
5
6
7
8
9
10
11
12
13
14
15
16
17
18
19
20
21
22
23
24
25
26
27
28
29
30
31
32
33
34
35
36
37
38

bifunctional amine catalyst

bifunctional binaphtholate catalyst

n = 1: **E1** (R = H), **E2** (R = CH₃)
E3 (R = CF₃), **E4** (R = I)
n = 2: **E5** (R = I)

entry	catalyst	solvent	ee (%) ^b	conv. (%) ^c	s ^d
1 ^e	A	<i>o</i> -xylene	68	54	7
2 ^e	B	<i>o</i> -xylene	-5	11	2
3 ^e	C	<i>o</i> -xylene	12	33	2
4 ^e	D	<i>o</i> -xylene	36	31	13
5	E1	<i>o</i> -xylene	2	13	1
6	E2	<i>o</i> -xylene	98	57	30
7	E3	<i>o</i> -xylene	95	54	35
8	E4	<i>o</i> -xylene	90	52	32
9	E5	<i>o</i> -xylene	-	<5	-
10	F	<i>o</i> -xylene	98	54	50
11	G	<i>o</i> -xylene	57	49	7
12	F	DCM	98	57	30
13	F	EA	23	47	2
14	F	Et ₂ O	97	52	76
15	F	1,4-dioxane	-	<5	-
16	F	THF	-	<5	-
17	F	anisole	96	57	24
18	F	cyclopentyl methyl ether	76	52	13
19	F	di- <i>n</i> -butyl ether	98	52	91
20	F	MTBE	82	51	21
21 ^f	F	di- <i>n</i> -butyl ether	95	50	146
22 ^{f,g}	F	di- <i>n</i> -butyl ether	95	49	263
23 ^{f,h}	F	di- <i>n</i> -butyl ether	12	11	97

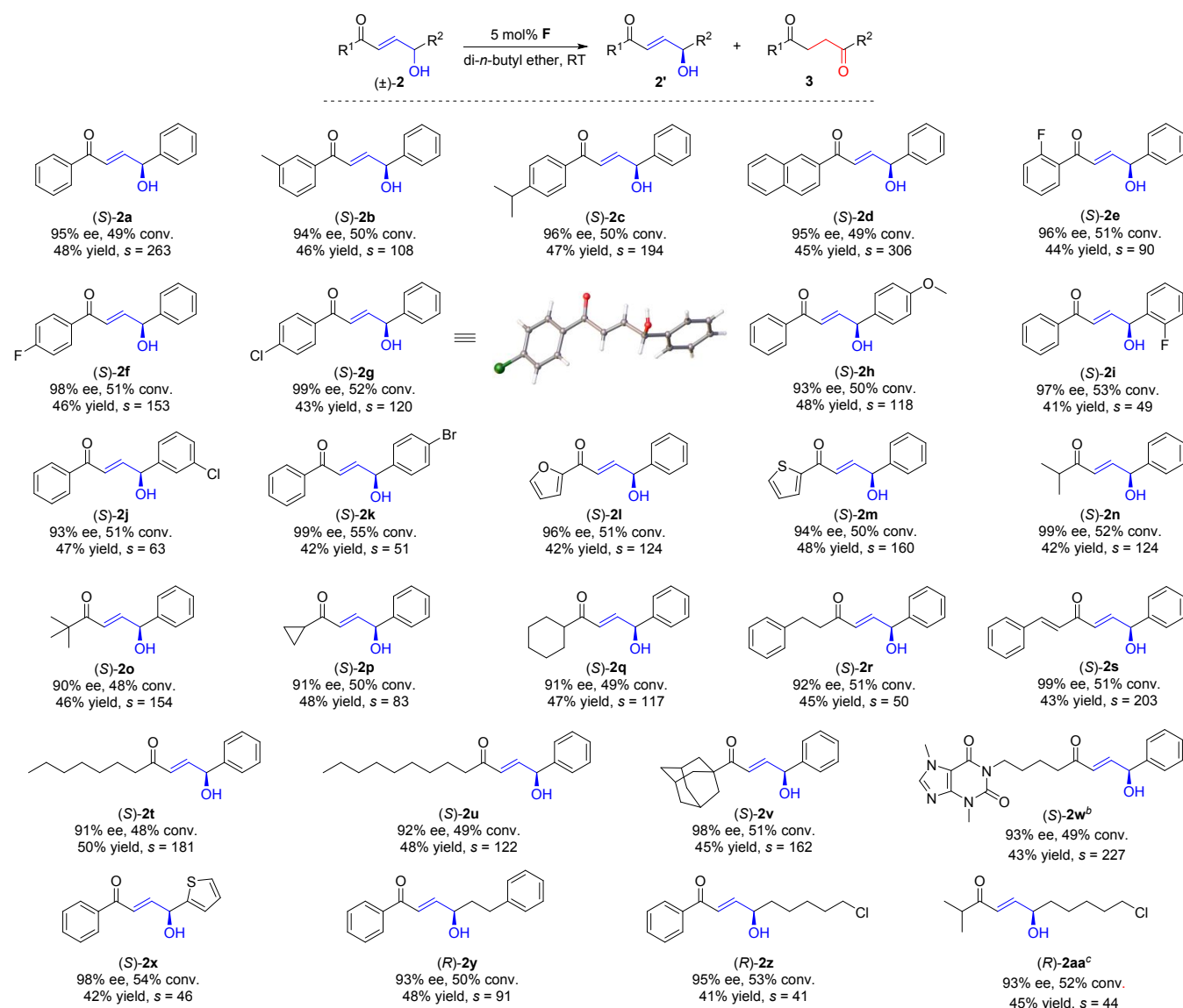
^aReaction conditions: (±)-**2a** (0.1 mmol), catalyst (0.01 mmol) in the solvent (1.0 mL) at RT for 3 h, unless otherwise specified.

^bEnantiomeric excesses were determined by HPLC analysis. ^cConversion ratio was determined by ¹H NMR spectroscopy. ^dThe selectivity factors were calculated by the methods of Fiaud: $s = \ln[(1-\text{Conv.})(1-ee)]/\ln[(1-\text{Conv.})(1+ee)]$. All the reported *s* factors were an average of 3 repeats. ^e12 h reaction time. ^f1.5 mL of di-*n*-butyl ether. ^g5 mol% catalyst loading. ^h1 mol% catalyst loading.

catalysts resulted in significantly higher catalytic activity and enantioselectivity (entries 6, 7 and 8). The ether chain length was also shown to play a crucial role in the performance of the catalyst, which, as would be expected, is responsible for the formation of a suitable chiral coordination cage with potassium cation. The catalyst bearing longer (n = 2) ether units showed almost no activity (Table 1, entry 9). Finally, catalysts F and G with the substituents at the C₁ position of the chain were tested (Table 1, entries 10 and 11). A comparison of catalysts E-G illustrated that the presence of substituents at the C₁ position of the chain affected the catalytic performance. Gratifyingly, catalyst F with the phenyl rings at the C₁ position of the chain showed the highest *s* factor (*s* factor = 50 at 54% conversion) and was selected for further

optimization. Afterward, changing the solvent from *o*-xylene to ether gave an improved enantioselectivity, whereas 1,4-dioxane and THF resulted in the poor conversion and the non-measurable degree of selectivity. Finally, di-*n*-butyl ether was confirmed as the ideal solvent for recovering (S)-**2a** with the excellent selectivity and enantioselectivity (Table 1, entry 21). This high level of selectivity could be maintained with lower catalyst loading (Table 1, entries 22 and 23). Even with catalyst loading of 1 mol%, excellent *s*-factor was obtained (*s* = 97 in Table 1, entry 23).

Next, the scope of the reaction was examined among a range of racemic allylic alcohols under the optimized conditions (Table 2). Generally, most of the recovered

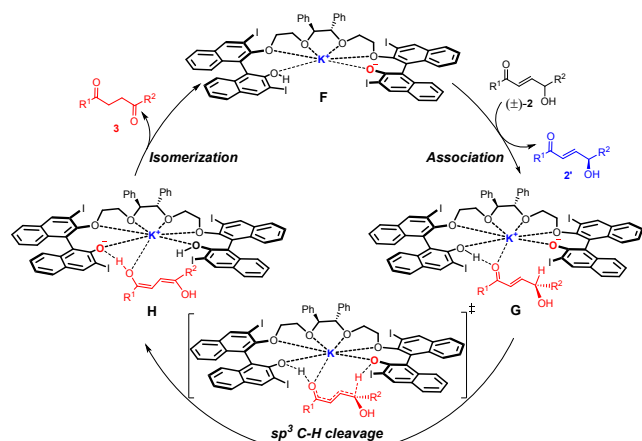
Table 2. Substrate Scope^a

^aUnless otherwise indicated, the reactions were carried out with (**±**-**2**) (0.1 mmol), **F** (5 mol%) in di-*n*-butyl ether (1.5 mL) at RT, please see Supporting Information for reaction time. Enantiomeric excesses were determined by HPLC analysis; conversion ratio was determined by ¹H NMR spectroscopy; isolated yield; the selectivity factors were calculated by the methods of Fiaud: $s = \ln[(1-\text{Conv.})(1-ee)]/\ln[(1-\text{Conv.})(1+ee)]$, all the reported *s* factors were an average of 3 repeats. ^bDi-*n*-butyl ether/DCM (0.75 mL/0.75 mL) as solvent. ^cPerformed at 55 °C.

allylic alcohols were obtained with excellent ee values and high *s* factors. The functional groups on the phenyl ring at R¹ and/or R² position, such as methyl, isopropyl, methoxyl, and halogen groups, were well tolerant to current reaction systems, thus giving the corresponding products (**S**)-**2a-2k** in excellent enantioselectivities and good yields. The substrates bearing heterocyclic and alkyl substituents at R¹ position also led to the excellent selectivity ((**S**)-**2l-2w**). Our protocol was also found to be general with diverse R² moieties. The substrates having heteroaromatic as well as alkyl moiety at R² afforded the desired products, (**S**)-**2x** and (**R**)-**2y-2aa**, respectively, with excellent enantioselectivity. The relative and absolute configurations of (**S**)-**2g** were unambiguously established by X-ray crystallographic analysis.¹⁸

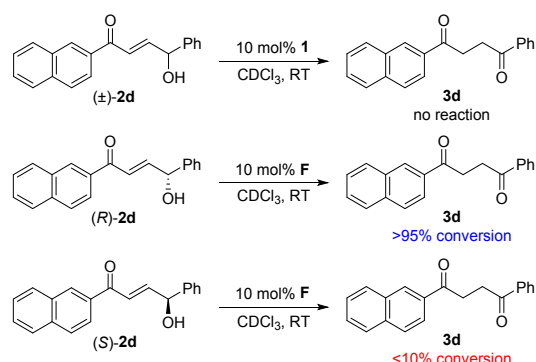
Based on our experimental findings, a postulated reaction pathway for this kinetic resolution is depicted in Scheme 4. The chiral Brønsted base catalyst **F** might be associated with substrates (**R**)-**2a** (R¹ = R² = Ph) to generate intermediate **G** by hydrogen bonding. The subsequent sp³ C-H bond cleavage of intermediate **G** afforded bis-enol intermediate **H**. The isomerization of bis-enol intermediate **H** gave the kinetic product **3a** together with the regeneration of the chiral Brønsted base catalyst **F**, whereas the isomerization of (**S**)-**2a** (R¹ = R² = Ph) occurred at a relatively low rate due to the higher activation energy of the cleavage of the sp³ C-H bond between the chiral Brønsted base catalyst **F** and (**S**)-**2a**, thus leaving the unreactive (**S**)-**2a**.

Scheme 4. Proposed Reaction Pathway



To confirm our proposed mechanism, a series of control experiments were performed. Firstly, the background reaction was tested. In the presence of catalyst **1**, the reaction did not proceed at all under the optimized reaction conditions, demonstrating that **F** played a crucial role in this reaction. Next, we performed the reaction with optically pure **2d** as the substrate. As shown in Scheme 5, the reaction of (*R*)-**2d** (99% ee) gave **3d** in the excellent yield under the optimized reaction conditions (see Supporting Information, Figure S2). However, the isomerization of (*S*)-**2d** (99% ee) proceeded sluggishly (see Supporting Information, Figure S3). These control experiments further confirmed that (*R*)-**2d** had a faster reaction rate than (*S*)-**2d**.

Scheme 5. Control Experiments



To gain further insights into the mechanism of this transformation, we measured the independent initial rates on parallel reactions with substrates (*±*)-**2d** and (*±*)-**2d-D** under the optimized reaction conditions (Scheme 6), which resulted in a strong primary intermolecular KIE¹⁹ (5.1 ± 0.2), strongly suggesting that the deprotonation of allylic C-H was involved in the rate-determining step.

Scheme 6. Kinetic Isotopic Effect

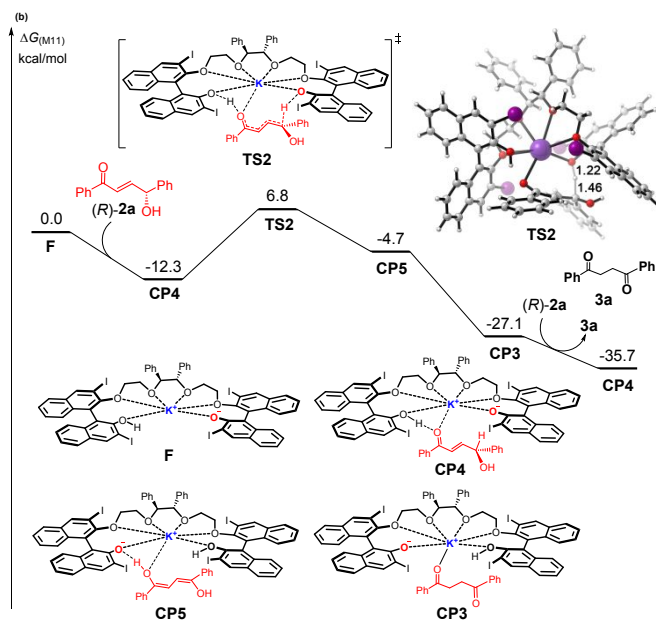
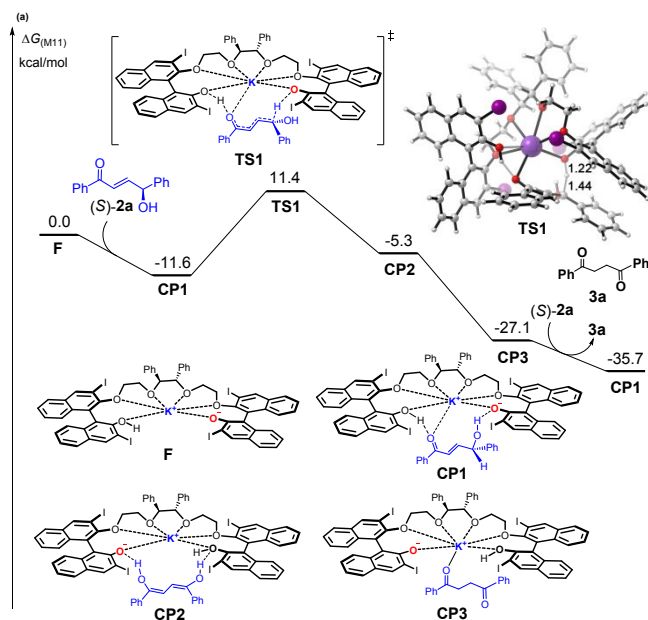
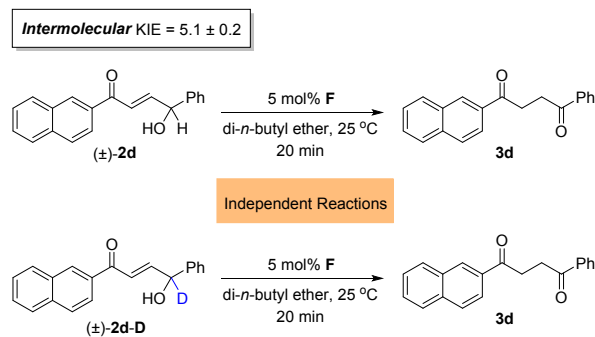


Figure 1. (a) Free energy profile and structural information of the reaction pathway with (*S*)-**2a** as the substrate. (b) Calculated free energy profiles of the reaction pathway with (*R*)-**2a** as the substrate. The values of bond lengths are given in angstroms.

To elucidate the mechanism, density functional theory (DFT) method M11 was employed to study the mechanism of the chiral BINOL-based alkoxides catalyzed kinetic resolution of allylic alcohol.²⁰ The calculated free energy profile for the reaction pathway with (*S*)-**2a** as the substrate is shown in Figure 1a. The coordination of (*S*)-**2a** to the active catalyst **F** with hydrogen bond interaction formed intermediate **CP1** with 11.6 kcal/mol exothermic. The subsequent intramolecular deprotonation, which gave the bis-enol intermediate **CP2**, occurred via the transition state **TS1** with an overall barrier of 23.0 kcal/mol. The structural information of the transition state **TS1** showed that the bond lengths of the breaking C-H bond and the forming O-H bond were 1.44 and 1.22 Å, respectively. The isomerization of the bis-enol intermediate **CP2** gave the 1,4-diketone intermediate **CP3**. The subsequent ligand exchange between **CP3** and (*S*)-**2a** generated the final product **3a** and **CP1** to complete the catalytic cycle.

The calculated free energy profile of the reaction pathway with (*R*)-**2a** as the substrate is shown in Figure 1b. The overall activation barrier for the intramolecular deprotonation transition state **TS2** is 19.1 kcal/mol, which is 3.9 kcal/mol lower than that of **TS1**. In transition state **TS2**, the bond lengths of the breaking C-H bond and the forming O-H bond are 1.46 and 1.22 Å, respectively. The calculated results indicated that the chiral active catalyst **F** reacted with (*R*)-**2a** to give the 1,4-diketone product **3a**, whereas (*S*)-**2a** would not be transformed into 1,4-diketone product due to the high activation energy of the transition state **TS1**.

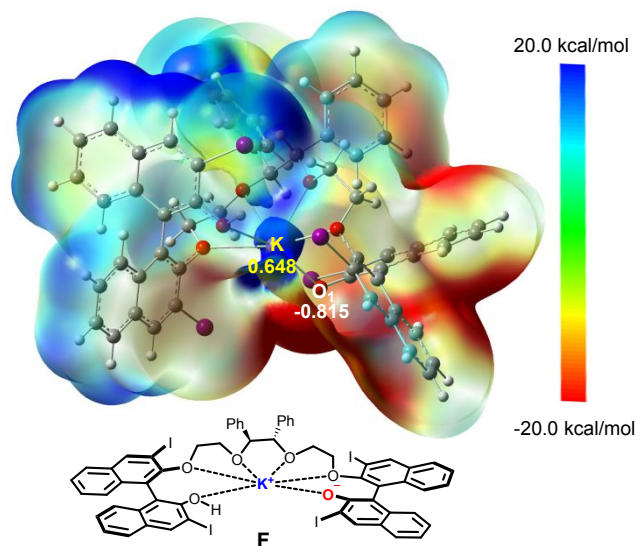


Figure 2. Electrostatic potential maps and the total natural population analysis charges of certain atoms in catalyst **F**.

To obtain more information for the active catalyst, natural population analysis (NPA) towards catalyst **F** was performed. The NPA charge value of certain atoms shown in Figure 2 suggested that the negative charges of the catalyst **F** were mainly located at the naphthalen-2-olate. The charge of the oxygen atom (O_i) in naphthalen-2-olate was -0.815, whereas the charge of the potassium atom was

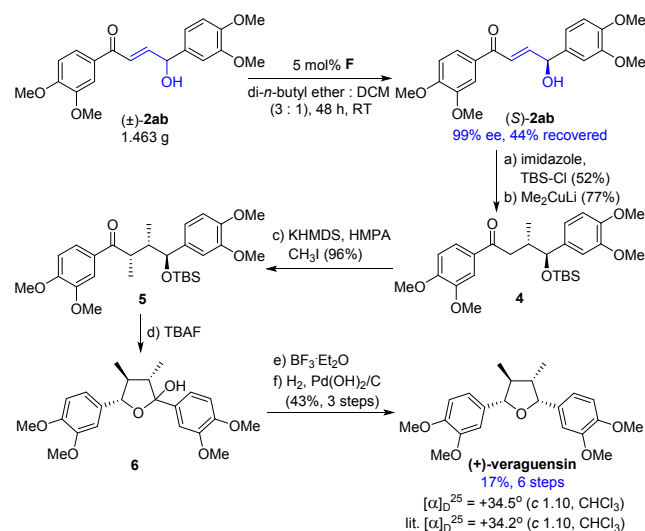
0.648. The natural population analysis indicated that the active site for **F** was the oxygen atom (O_i) in naphthalen-2-olate, which underwent the deprotonation of C-H bond in (*R*)-**2a**.

Table 3. Distortion Energies and Interaction Energies of the Transition States **TS1** and **TS2** Calculated by the B₃LYP/6-31G(d) Method

	$\Delta E^{\ddagger}_{dist(2a)}$	$\Delta E^{\ddagger}_{dist(F)}$	$\Delta E^{\ddagger}_{dist}$	$\Delta E^{\ddagger}_{int}$	ΔE^{\ddagger}
TS1	41.3	11.6	52.9	-49.7	3.2
TS2	32.9	11.1	44.0	-46.1	-2.0

The distortion-interaction energy analysis²¹ was employed to explain the reactivity trends of the kinetic resolution. As shown in Table 3, the total activation energy (ΔE^{\ddagger}) is devolved into the sum of distortion energy ($\Delta E^{\ddagger}_{dist}$) and interaction energy ($\Delta E^{\ddagger}_{int}$) between distorted reactants. According to B₃LYP calculations of **TS1**, the distortion energy was 52.9 kcal/mol and the interaction energy was -49.7 kcal/mol. The distortion energy for **TS2** was 44.0 kcal/mol, which was 8.9 kcal/mol lower than that of **TS1**. The interaction energies of those two transition states were close. Distortion-interaction energy analysis indicated that the reactivity of the deprotonation of (*S*)-**2a** and (*R*)-**2a** was controlled by the distortion energy resulting from the difference in the distortion energy between (*S*)-**2a** and (*R*)-**2a**.

Scheme 7. Asymmetric Synthesis of (+)-Veraguensin^a



^aReagents and conditions: (a) imidazole, TBS-Cl, DMF, 40 °C, 1 h, 52%; (b) Me₂CuLi, THF, -40 °C, 1 h, 77%; (c) KHMDS, HMPA, CH₃I, THF, -78 °C, 40 min, 96%; (d) TBAF, THF, RT, 15 h; (e) BF₃·Et₂O, toluene, RT, 10 min; (f) H₂, Pd(OH)₂/C, EtOAc, RT, 12 h, 43% for three steps.

Optically active allylic alcohols are versatile building blocks for the synthesis of natural products and pharmaceuticals. For example, they are key intermediates for the synthesis of natural products such as (+)-veraguensin, (+)-verrucosin, (+)-calopiptin, and (-)-

virgatusin.²² To further illustrate the generality and synthetic utility of this methodology, we synthesized the natural product (+)-veraguensin with this transformation as a key step. (+)-Veraguensin was first isolated from the Mexican tree *Ocotea veragzlenis* Mez. and exhibited the significant neurite outgrowth promoting effect in primary-cultured rat cortical neurons and NGF-differentiated PC12 cells and protective effects against cell death induced by several insults. Starting from (*S*)-**2ab**, we synthesized (+)-veraguensin in 17% overall yield in six steps, including the following key reactions. Firstly, after *anti*-selective Michael addition to γ -oxyenone, *syn*-selective α -methylation of the resulting ketone generated the intermediate **5**. Secondly, upon the treatment with TBAF, the resulting ketol was immediately cyclized to give hemiacetal **6** as a single isomer, which was hydrogenated on Pd(OH)₂ in EtOAc to give (+)-veraguensin.

CONCLUSIONS

In conclusion, we developed an efficient chiral BINOL derivatives-based alkoxide, which was used as the Brønsted base catalyst for kinetic resolution of racemic allylic alcohols through asymmetric isomerization. This method represented a new approach for the preparation of optically active allylic alcohols in excellent enantioselectivities. An exhaustive ¹H NMR mechanistic study, deuterium incorporation experiments and DFT calculation indicated that the deprotonation of allylic C-H was probably involved in the rate-determining step. With this transformation as a key step, we achieved the asymmetric synthesis of bioactive natural product (+)-veraguensin.

ASSOCIATED CONTENT

Supporting Information.

Experimental procedure and characterization data for all the products. This material is available free of charge via the Internet at <http://pubs.acs.org>.

AUTHOR INFORMATION

Corresponding Authors

*yhl198151@cqu.edu.cn

*lanyu@cqu.edu.cn

Author Contributions

†Y.L. and S.L. contributed equally.

Notes

The authors declare no competing financial interest.

ACKNOWLEDGMENTS

This study was supported by the Fundamental Research Funds for the Central Universities in China (Grant CQDXWL-2014-Z003 and 2018CDXZ0002), the Scientific Research Foundation of China (Grant 21772018, 21822303, and 21772020), and the Ministry of Science, ICT, and Future Planning in Korea (Grant NRF-2014R1A2A1A01005794 and NRF-2016-R1A4A101451).

REFERENCES

(1) For selected reviews, see: (a) Seayad, J.; List, B. Asymmetric organocatalysis. *Org. Biomol. Chem.* **2005**, *3*, 719–724. (b) Pellissier, H. Asymmetric organocatalysis. *Tetrahedron* **2007**, *63*, 9267–9331. (c) Dondoni, A.; Massi, A. Asymmetric organocatalysis: from infancy to adolescence. *Angew. Chem., Int. Ed.* **2008**, *47*, 4638–4660. (d) Marqués-López, E.; Herrera, R. P.; Christmann, M. Asymmetric organocatalysis in total synthesis – a trial by fire. *Nat. Prod. Rep.* **2010**, *27*, 1138–1167. (e) Giacalone, F.; Gruttadauria, M.; Agrigento, P.; Noto, R. Low-loading asymmetric organocatalysis. *Chem. Soc. Rev.* **2012**, *41*, 2406–2447. (f) Alemán, J.; Cabrera, S. Applications of asymmetric organocatalysis in medicinal chemistry. *Chem. Soc. Rev.* **2013**, *42*, 774–793. (g) Volla, C. M. R.; Atodiresei, I.; Rueping, M. Catalytic C – C bond-forming multi-component cascade or domino reactions: pushing the boundaries of complexity in asymmetric organocatalysis. *Chem. Rev.* **2014**, *14*, 2390–2431. (h) Atodiresei, I.; Vila, C.; Rueping, M. Asymmetric organocatalysis in continuous flow: opportunities for impacting industrial catalysis. *ACS Catal.* **2015**, *5*, 1972–1985.

(2) For selected book and reviews, see: (a) Ting, A.; Schaus, S. E. Brønsted Bases. In *Comprehensive Enantioselective Organocatalysis: Catalysts, Reactions, and Applications*; Dalko, P. I., Ed.; Wiley-VCH: Weinheim, 2013; Vol. 2, pp 343–363. (b) O'Brien, P. Recent advances in asymmetric synthesis using chiral lithium amide bases. *J. Chem. Soc., Perkin Trans. 1* **1998**, 1439–1457. (c) Shibasaki, M.; Yoshikawa, N. Lanthanide complexes in multifunctional asymmetric catalysis. *Chem. Rev.* **2002**, *102*, 2187–2209. (d) Collum, D. B.; McNeil, A. J.; Ramirez, A. Lithium diisopropylamide: solution kinetics and implications for organic synthesis. *Angew. Chem., Int. Ed.* **2007**, *46*, 3002–3017. (e) Yamashita, Y.; Tsubogo, T.; Kobayashi, S. Chiral alkaline-earth metal catalysts for asymmetric bond-forming reactions. *Chem. Sci.* **2012**, *3*, 967–975. (f) Teng, B.; Lim, W. C.; Tan, C.-H. Recent advances in enantioselective Brønsted base organocatalytic reactions. *Synlett* **2017**, *28*, 1272–1277.

(3) For selected books and reviews, see: (a) Inokuma, T.; Takemoto, Y. In *Science of Synthesis, Asymmetric Organocatalysis*; List, B., Maruoka, K., Eds.; Thieme: Stuttgart, 2012; Vol. 2, pp 437–497. (b) Jang, H. B.; Oh, J. S.; Song, C. E. In *Science of Synthesis, Asymmetric Organocatalysis*; List, B., Maruoka, K., Eds.; Thieme: Stuttgart, 2012; Vol. 2, pp 119–168. (c) Singh, R. P.; Deng, L. In *Science of Synthesis, Asymmetric Organocatalysis*; List, B., Maruoka, K., Eds.; Thieme: Stuttgart, 2012; Vol. 2, pp 41–117. (d) Marcelli, T.; van Maarseveen, J. H.; Hiemstra, H. Cupreines and cupreidines: an emerging class of bifunctional cinchona organocatalysts. *Angew. Chem., Int. Ed.* **2006**, *45*, 7496–7504. (e) Connon, S. J. Asymmetric catalysis with bifunctional cinchona alkaloid-based urea and thiourea organocatalysts. *Chem. Commun.* **2008**, 2499–2510. (f) Palomo, C.; Oiarbide, M.; López, R. Asymmetric organocatalysis by chiral Brønsted bases: implications and applications. *Chem. Soc. Rev.* **2009**, *38*, 632–653. (g) Chauhan, P.; Chimni, S. S. Aromatic hydroxyl group—a hydrogen bonding activator in bifunctional asymmetric organocatalysis. *RSC Adv.* **2012**, *2*, 737–758. (h) Fang, X.; Wang, C.-J. Recent advances in asymmetric organocatalysis mediated by bifunctional amine – thioureas bearing multiple hydrogen-bonding donors. *Chem. Commun.* **2015**, *51*, 1185–1197.

(4) For selected book and reviews, see: (a) Shibasaki, M.; Matsunaga, S. In *Privileged Chiral Ligands and Catalysts*; Zhou, Q.-L., Ed.; Wiley-VCH: Weinheim, 2011; Vol. 8, pp 295–332. (b) Chen, Y.; Yekta, S.; Yudin, A. K. Modified BINOL ligands in asymmetric catalysis. *Chem. Rev.* **2003**, *103*, 3155–3211. (c) Brunel, J. M. BINOL: A versatile chiral reagent. *Chem. Rev.* **2005**, *105*, 857–897. (d) Shibasaki, M.; Matsunaga, S. Design and application of linked-BINOL chiral ligands in bifunctional asymmetric catalysis. *Chem. Soc. Rev.* **2006**, *35*, 269–279. (e) Parmar, D.;

Sugiono, E.; Raja, S.; Rueping, M. Complete field guide to asymmetric BINOL-phosphate derived Brønsted acid and metal catalysis: history and classification by mode of activation; Brønsted acidity, hydrogen bonding, ion pairing, and metal phosphates. *Chem. Rev.* **2014**, *114*, 9047–9153.

(5) (a) Brønsted, J. N. Some Remarks on the concept of acids and bases. *Rec. Trav. Chim. Pays Bas* **1923**, *42*, 718–728 (German title: Einige bemerkungen über den begriff der säuren und basen). (b) Brønsted, J. N. The acid-basic function of molecules and its dependency on the electric charge type. *J. Phys. Chem.* **1925**, *30*, 777–790. (c) Brønsted, J. N. Theory of the acidic-basic function. *Ber. Dtsch. Chem. Ges. B* **1928**, *61*, 2049–2063 (German title: Zur theorie der saure-basen-funktion). (d) Brønsted, J. N. Acid and basic catalysis. *Chem. Rev.* **1928**, *5*, 231–338. (e) Lowry, T. M. The uniqueness of hydrogen. *J. Soc. Chem. Ind., London* **1923**, *42*, 43–47. (f) Lowry, T. M. Co-ordination and acidity. *J. Soc. Chem. Ind., London* **1923**, *42*, 1048–1052.

(6) (a) Schiffers, R.; Kagan, H. B. Asymmetric catalytic reduction of ketones with hypervalent trialkoxysilanes. *Synlett* **1997**, 1175–1178. (b) Holmes, I. P.; Kagan, H. B. The asymmetric addition of trimethylsilyl cyanide to aldehydes catalysed by anionic chiral nucleophiles. part 1. *Tetrahedron Lett.* **2000**, *41*, 7453–7456. (c) Nakajima, M.; Orito, Y.; Ishizuka, T.; Hashimoto, S. Enantioselective aldol reaction of trimethoxysilyl enol ether catalyzed by lithium binaphtholate. *Org. Lett.* **2004**, *6*, 3763–3765. (d) Hatano, M.; Ikeno, T.; Miyamoto, T.; Ishihara, K. Chiral lithium binaphtholate aqua complex as a highly effective asymmetric catalyst for cyanohydrin synthesis. *J. Am. Chem. Soc.* **2005**, *127*, 10776–10777. (e) Hatano, M.; Horibe, T.; Ishihara, K. Chiral lithium(I) binaphtholate salts for the enantioselective direct Mannich-type reaction with a change of syn/anti and absolute stereochemistry. *J. Am. Chem. Soc.* **2010**, *132*, 56–57. (f) Kotani, S.; Kukita, K.; Tanaka, K.; Ichibakase, T.; Nakajima, M. Lithium binaphtholate-catalyzed asymmetric addition of lithium acetylides to carbonyl compounds. *J. Org. Chem.* **2014**, *79*, 4817–4825. (g) Cai, H.; Nie, J.; Zheng, Y.; Ma, J.-A. Lithium binaphtholate-catalyzed enantioselective enyne addition to ketones: access to enynylated tertiary alcohols. *J. Org. Chem.* **2014**, *79*, 5484–5493. (h) Kotani, S.; Moritani, M.; Nakajima, M. Chiral lithium binaphtholate for enantioselective Michael addition of acyclic α -alkyl- β -keto esters to vinyl ketones. *Asian J. Org. Chem.* **2015**, *4*, 616–618.

(7) (a) Yan, H.; Jang, H. B.; Lee, J.-W.; Kim, H. K.; Lee, S. W.; Yang, J. W.; Song, C. E. A chiral-anion generator: application to catalytic desilylative kinetic resolution of silyl-protected secondary alcohols. *Angew. Chem., Int. Ed.* **2010**, *49*, 8915–8917. (b) Yan, H.; Oh, J. S.; Lee, J.-W.; Song, C. E. Scalable organocatalytic asymmetric Strecker reactions catalysed by a chiral cyanide generator. *Nat. Commun.* **2012**, *3*, 1212. (c) Park, S. Y.; Lee, J.-W.; Song, C. E. Parts-per-million level loading organocatalysed enantioselective silylation of alcohols. *Nat. Commun.* **2015**, *6*, 7512. (d) Li, L.; Liu, Y.; Peng, Y.; Yu, L.; Wu, X.; Yan, H. Kinetic resolution of β -sulfonyl ketones through enantioselective β -elimination using a cation-binding polyether catalyst. *Angew. Chem., Int. Ed.* **2016**, *55*, 331–335. (e) Liu, Y.; Ao, J.; Paladhi, S.; Song, C. E.; Yan, H. Organocatalytic asymmetric synthesis of chiral dioxazinanes and dioxazepanes with in situ generated nitrones via a tandem reaction pathway using a cooperative cation binding catalyst. *J. Am. Chem. Soc.* **2016**, *138*, 16486–16492. (f) Vaithyanathan, V.; Kim, M. J.; Liu, Y.; Yan, H.; Song, C. E. Direct access to chiral β -fluoroamines with quaternary stereogenic center through cooperative cation-binding catalysis. *Chem. - Eur. J.* **2017**, *23*, 1268–1272. (g) Kim, M. J.; Xue, L.; Liu, Y.; Paladhi, S.; Park, S. J.; Yan, H.; Song, C. E. Cooperative cation-binding catalysis as an efficient approach for enantioselective Friedel–Crafts reaction of indoles and pyrrole.

Adv. Synth. Catal. **2017**, *359*, 811–823. (h) Yu, L.; Wu, X.; Kim, M. J.; Vaithyanathan, V.; Liu, Y.; Tan, Y.; Qin, W.; Song, C. E.; Yan, H. Asymmetric synthesis of 2-thiocyanato-2-(1-aminoalkyl)-substituted 1-tetralones and 1-indanones with tetrasubstituted carbon stereogenic centers via cooperative cation-binding catalysis. *Adv. Synth. Catal.* **2017**, *359*, 1879–1891. (i) Park, S. Y.; Hwang, I.-S.; Lee, H.-J.; Song, C. E. Biomimetic catalytic transformation of toxic α -oxoaldehydes to high-value chiral α -hydroxythioesters using artificial glyoxalase I. *Nat. Commun.* **2017**, *8*, 14877. (j) Tan, Y.; Luo, S.; Li, D.; Zhang, N.; Jia, S.; Liu, Y.; Qin, W.; Song, C. E.; Yan, H. Enantioselective synthesis of *anti*-*syn*-trihalides and *anti*-*syn*-*anti*-tetrahalides via asymmetric β -elimination. *J. Am. Chem. Soc.* **2017**, *139*, 6431–6436. (k) Duan, M.; Liu, Y.; Ao, J.; Xue, L.; Luo, S.; Tan, Y.; Qin, W.; Song, C. E.; Yan, H. Asymmetric synthesis of trisubstituted tetrahydrothiophenes via in situ generated chiral fluoride-catalyzed cascade sulfa-Michael/Aldol reaction of 1,4-dithiane-2,5-diol and α,β -unsaturated ketones. *Org. Lett.* **2017**, *19*, 2298–2301. (l) Paladhi, S.; Liu, Y.; Kumar, B. S.; Jung, M.-J.; Park, S. Y.; Yan, H.; Song, C. E. Fluoride anions in self-assembled chiral cage for the enantioselective protonation of silyl enol ethers. *Org. Lett.* **2017**, *19*, 3279–3282. (m) Paladhi, S.; Park, S. Y.; Yang, J. W.; Song, C. E. Asymmetric synthesis of α -fluoro- β -amino-oxindoles with tetrasubstituted C–F stereogenic centers via cooperative cation-binding catalysis. *Org. Lett.* **2017**, *19*, 5336–5339. (n) Paladhi, S.; Hwang, I.-S.; Yoo, E. J.; Ryu, D. H.; Song, C. E. Kinetic resolution of β -hydroxy carbonyl compounds via enantioselective dehydration using a cation-binding catalyst: facile access to enantiopure chiral aldols. *Org. Lett.* **2018**, *20*, 2003–2006.

(8) For selected reviews and accounts, see: (a) van der Drift, R. C.; Bouwman, E.; Drent, E. Homogeneously catalysed isomerisation of allylic alcohols to carbonyl compounds. *J. Organomet. Chem.* **2002**, *650*, 1–24. (b) Uma, R.; Crévisy, C.; Grée, R. Transposition of allylic alcohols into carbonyl compounds mediated by transition metal complexes. *Chem. Rev.* **2003**, *103*, 27–51. (c) Cadierno, V.; Crochet, P.; Gimeno, J. Ruthenium-catalyzed isomerizations of allylic and propargylic alcohols in aqueous and organic media: applications in synthesis. *Synlett* **2008**, *2008*, 1105–1124. (d) Ahlsten, N.; Bartoszewicz, A.; Martín-Matute, B. Allylic alcohols as synthetic enolate equivalents: Isomerisation and tandem reactions catalysed by transition metal complexes. *Dalton Trans.* **2012**, *41*, 1660–1670. (e) Lorenzo-Luis, P.; Romerosa, A.; Serrano-Ruiz, M. Catalytic isomerization of allylic alcohols in water. *ACS Catal.* **2012**, *2*, 1079–1086. (f) Cahard, D.; Gaillard, S.; Renaud, J.-L. Asymmetric isomerization of allylic alcohols. *Tetrahedron Lett.* **2015**, *56*, 6159–6169. (g) Li, H.; Mazet, C. Iridium-catalyzed selective isomerization of primary allylic alcohols. *Acc. Chem. Res.* **2016**, *49*, 1232–1241.

(9) (a) Tanaka, K.; Qiao, S.; Tobisu, M.; Lo, M. M.-C.; Fu, G. C. Enantioselective isomerization of allylic alcohols catalyzed by a rhodium/phosphaferrocene complex. *J. Am. Chem. Soc.* **2000**, *122*, 9870–9871. (b) Tanaka, K.; Fu, G. C. A versatile new catalyst for the enantioselective isomerization of allylic alcohols to aldehydes: scope and mechanistic studies. *J. Org. Chem.* **2001**, *66*, 8177–8186.

(10) (a) Mantilli, L.; Gérard, D.; Torche, S.; Besnard, C.; Mazet, C. Iridium-catalyzed asymmetric isomerization of primary allylic alcohols. *Angew. Chem., Int. Ed.* **2009**, *48*, 5143–5147. (b) Mantilli, L.; Mazet, C. Expanded scope for the iridium-catalyzed asymmetric isomerization of primary allylic alcohols using readily accessible second-generation catalysts. *Chem. Commun.* **2010**, *46*, 445–447.

(11) (a) Li, J.-Q.; Peters, B.; Andersson, P. G. Highly enantioselective asymmetric isomerization of primary allylic

alcohols with an iridium–N,P complex. *Chem. - Eur. J.* **2011**, *17*, 1143–1145. (b) Wu, R.; Beauchamps, M. G.; Laquidara, J. M.; Sowa Jr., J. R. Ruthenium-catalyzed asymmetric transfer hydrogenation of allylic alcohols by an enantioselective isomerization/transfer hydrogenation mechanism. *Angew. Chem., Int. Ed.* **2012**, *51*, 2106–2110. (c) Arai, N.; Sato, K.; Azuma, K.; Ohkuma, T. Enantioselective isomerization of primary allylic alcohols into chiral aldehydes with the tolbinap/dbapen/ruthenium(II) catalyst. *Angew. Chem., Int. Ed.* **2013**, *52*, 7500–7504.

(12) For selected book and reviews on kinetic resolution, see: (a) Kagan, H. B.; Fiaud, J. C. Kinetic Resolution. In *Topics in Stereochemistry*; Eliel, E. L., Wilen, S. H., Eds.; John Wiley & Sons: Canada, 1988; Vol. 18, pp 249–330. (b) Keith, J. M.; Larrow, J. F.; Jacobsen, E. N. Practical considerations in kinetic resolution reactions. *Adv. Synth. Catal.* **2001**, *343*, 5–26. (c) Vedejs, E.; Jure, M. Efficiency in nonenzymatic kinetic resolution. *Angew. Chem., Int. Ed.* **2005**, *44*, 3974–4001.

(13) For selected examples, see: (a) Kitamura, M.; Manabe, K.; Noyori, R.; Takaya, H. Kinetic resolution of 4-hydroxy-2-cyclopentenone by rhodium-catalyzed asymmetric isomerization. *Tetrahedron Lett.* **1987**, *28*, 4719–4720. (b) Hiroya, K.; Kurihara, Y.; Ogasawara, K. Asymmetrization of meso 1,4-enediol ethers by isomerization with a chiral binap-Rh^I catalyst. *Angew. Chem., Int. Ed. Engl.* **1995**, *34*, 2287–2289. (c) Ito, M.; Kitahara, S.; Ikariya, T. Cp*⁺Ru(PN) complex-catalyzed isomerization of allylic alcohols and its application to the asymmetric synthesis of Muscone. *J. Am. Chem. Soc.* **2005**, *127*, 6172–6173. (d) Ren, K.; Zhang, L.; Hu, B.; Zhao, M.; Tu, Y.; Xie, X.; Zhang, T. Y.; Zhang, Z. Cationic-rhodium-catalyzed kinetic resolution of allylic alcohols through a redox isomerization reaction in a noncoordinating solvent. *ChemCatChem* **2013**, *5*, 1317–1320. (e) Ren, K.; Zhao, M.; Hu, B.; Lu, B.; Xie, X.; Ratovelomanana-Vidal, V.; Zhang, Z. An enantioselective approach to 4-*O*-protected-2-cyclopentene-1,4-diol derivatives via a rhodium-catalyzed redox-isomerization reaction. *J. Org. Chem.* **2015**, *80*, 12572–12579.

(14) For selected examples, see: (a) Bizet, V.; Pannecoucke, X.; Renaud, J.-L.; Cahard, D. Ruthenium-catalyzed redox isomerization of trifluoromethylated allylic alcohols: mechanistic evidence for an enantiospecific pathway. *Angew. Chem., Int. Ed.* **2012**, *51*, 6467–6470. (b) Li, H.; Mazet, C. Catalyst-directed diastereoselective isomerization of allylic alcohols for the stereoselective construction of C(20) in steroid side chains: scope and topological diversification. *J. Am. Chem. Soc.* **2015**, *137*, 10720–10727. (c) Martinez-Erro, S.; Sanz-Marco, A.; Gómez, A. B.; Vázquez-Romero, A.; Ahlquist, M. S. G.; Martín-Matute, B. Base-catalyzed stereospecific isomerization of electron-deficient allylic alcohols and ethers through ion-pairing. *J. Am. Chem. Soc.* **2016**, *138*, 13408–13414.

(15) Liu, T.-L.; Ng, T. W.; Zhao, Y. Rhodium-catalyzed enantioselective isomerization of secondary allylic alcohols. *J. Am. Chem. Soc.* **2017**, *139*, 3643–3646.

(16) (a) Lumbroso, A.; Cooke, M. L.; Breit, B. Catalytic asymmetric synthesis of allylic alcohols and derivatives and their applications in organic synthesis. *Angew. Chem., Int. Ed.* **2013**, *52*, 1890–1932. (b) Volchkov, I.; Lee, D. Recent developments of

direct rhenium-catalyzed [1,3]-transpositions of allylic alcohols and their silyl ethers. *Chem. Soc. Rev.* **2014**, *43*, 4381–4394.

(17) *Cinchona Alkaloids in Synthesis and Catalysis: Ligands, Immobilization and Organocatalysis*; Song, C. E., Ed.; Wiley-VCH: Weinheim, 2009.

(18) CCDC 1554627 contains the supplementary crystallographic data for compound (S)-**2g**. (see Supporting Information).

(19) Simmons, E. M.; Hartwig, J. F. On the interpretation of deuterium kinetic isotope effects in C–H bond functionalizations by transition-metal complexes. *Angew. Chem., Int. Ed.* **2012**, *51*, 3066–3072.

(20) (a) Peverati, R.; Truhlar, D. G. Improving the accuracy of hybrid meta-GGA density functionals by range separation. *J. Phys. Chem. Lett.* **2011**, *2*, 2810–2817. (b) Qi, X.; Zhang, H.; Shao, A.; Zhu, L.; Xu, T.; Gao, M.; Liu, C.; Lan, Y. Silver migration facilitates isocyanide-alkyne [3 + 2] cycloaddition reactions: combined experimental and theoretical study. *ACS Catal.* **2015**, *5*, 6640–6647. (c) Qi, X.; Liu, S.; Zhang, T.; Long, R.; Huang, J.; Gong, J.; Yang, Z.; Lan, Y. Effective chirality transfer in [3+2] reaction between allenyl-rhodium and enal: mechanistic study based on DFT calculations. *J. Org. Chem.* **2016**, *81*, 8306–8311. (d) Liu, S.; Qi, X.; Qu, L.-B.; Bai, R.; Lan, Y. C–H bond cleavage occurring on a Rh(V) intermediate: a theoretical study of Rh-catalyzed arene azidation. *Catal. Sci. Technol.* **2018**, *8*, 1645–1651. (e) Long, R.; Huang, J.; Shao, W.; Liu, S.; Lan, Y.; Gong, J.; Yang, Z. Asymmetric total synthesis of (-)-lingzhiol via a Rh-catalysed [3+2] cycloaddition. *Nat. Commun.* **2014**, *5*, 5707.

(21) (a) Ess, D. H.; Houk, K. N. Distortion/interaction energy control of 1,3-dipolar cycloaddition reactivity. *J. Am. Chem. Soc.* **2007**, *129*, 10646–10647. (b) Lan, Y.; Wheeler, S. E.; Houk, K. N. Extraordinary difference in reactivity of ozone (OOO) and sulfur dioxide (OSO): a theoretical study. *J. Chem. Theory Comput.* **2011**, *7*, 2104–2111. (c) Ess, D. H. Distortion, interaction, and conceptual DFT perspectives of MO₄-alkene (M = Os, Re, Tc, Mn) cycloadditions. *J. Org. Chem.* **2009**, *74*, 1498–1508. (d) Liu, S.; Lei, Y.; Qi, X.; Lan, Y. Reactivity for the Diels–Alder reaction of cumulenes: a distortion–interaction analysis along the reaction pathway. *J. Phys. Chem. A* **2014**, *118*, 2638–2645.

(22) (a) Kitamura, M.; Hayashi, H.; Yano, M.; Tanaka, T.; Maezaki, N. A stereocontrolled construction of *rel*-(7*S*,8*S*,7'*R*,8'*S*)-7,7'-epoxylignan skeleton. *Heterocycles* **2007**, *71*, 2669–2680. (b) Kim, H.; Wooten, C. M.; Park, Y.; Hong, J. Stereoselective synthesis of tetrahydrofuran lignans via BF₃·OEt₂-promoted reductive deoxygenation/epimerization of cyclic hemiketal: synthesis of (-)-odoratisol C, (-)-futokadsurin A, (-)-veraguensin, (+)-fragransin A₂, (+)-galbelgin, and (+)-talaumidin. *Org. Lett.* **2007**, *9*, 3965–3968. (c) Matcha, K.; Ghosh, S. An asymmetric route to total synthesis of the furano lignan (+)-veraguensin. *Tetrahedron Lett.* **2010**, *51*, 6924–6927. (d) Harada, K.; Kubo, M.; Horiuchi, H.; Ishii, A.; Esumi, T.; Hioki, H.; Fukuyama, Y. Systematic asymmetric synthesis of all diastereomers of (-)-talaumidin and their neurotrophic activity. *J. Org. Chem.* **2015**, *80*, 7076–7088. (e) Chaimanee, S.; Pohmakotr, M.; Kuhakarn, C.; Reutrakul, V.; Soorukram, D. Asymmetric synthesis of *ent*-fragransin C₁. *Org. Biomol. Chem.* **2017**, *15*, 3985–3994.

Insert Table of Contents artwork here

